Geoscience Frontiers 7 (2016) 783–791

HOSTED BY

ELSEVIER

Contents lists available at ScienceDirect

China University of Geosciences (Beijing)

Geoscience Frontiers

journal homepage: www.elsevier.com/locate/gsf

Research paper

Tectonic significance of dykes in the Sarnu-Dandali alkaline complex, Rajasthan, northwestern Deccan Traps

Anjali Vijayan [a], Hetu Sheth [a,*], Kamal Kant Sharma [b]

[a] Department of Earth Sciences, Indian Institute of Technology Bombay (IITB), Powai, Mumbai 400076, India
[b] Department of Geology, Government Postgraduate College, Sirohi 307001, Rajasthan, India

ARTICLE INFO

Article history:
Received 9 July 2015
Received in revised form
20 August 2015
Accepted 4 September 2015
Available online 9 October 2015

Keywords:
Dyke swarms
Alkaline magmatism
Deccan Traps
Sarnu-Dandali
Barmer-Cambay rift

ABSTRACT

Whether swarms of preferentially oriented dykes are controlled by regional stress fields, or passively exploit basement structural fabric, is a much debated question, with support for either scenario in individual case studies. The Sarnu-Dandali alkaline complex, near the northwestern limit of the Deccan Traps continental flood basalt province, contains mafic to felsic alkaline volcano-plutonic rocks and carbonatites. The complex is situated near the northern end of the 600 km long, NNW–SSE-trending Barmer-Cambay rift. Mafic enclave swarms in the syenites suggest synplutonic mafic dykes injected into a largely liquid felsic magma chamber. Later coherent dykes in the complex, of all compositions and sizes, dominantly strike NNW–SSE, parallel to the Barmer-Cambay rift. The rift formed during two distinct episodes of extension, NW–SE in the early Cretaceous and NE–SW in the late Cretaceous. Control of the southern Indian Dharwar structural fabric on the rift trend, as speculated previously, is untenable, whereas the regional Precambrian basement trends (Aravalli and Malani) run NE–SW and NNE–SSW. We therefore suggest that the small-scale Sarnu-Dandali dykes and the much larger-scale Barmer-Cambay rift were not controlled by basement structure, but related to contemporaneous, late Cretaceous regional ENE–WSW extension, for which there is varied independent evidence.

1. Introduction

Dykes are planar conduits which transport magma from the zones of partial melting to higher-level magma chambers, and whereas many dykes originating from such chambers reach the Earth's surface, feeding volcanic eruptions (e.g., Gudmundsson, 1995), many more become arrested during ascent in the crust (Gudmundsson and Marinoni, 2002). Dykes are typically emplaced perpendicular to the regional minimum principal compressive stress σ_3 and thus serve as useful palaeostress indicators (e.g., Pollard, 1987; Gudmundsson and Marinoni, 2002; Tibaldi, 2015). However, dykes may also passively exploit pre-existing lines of weakness or structural fabric in their basement rocks, without any control by the regional stress field (e.g., Delaney et al., 1986; Baer et al., 1994; Mège and Korme, 2004). Identifying which of these two scenarios of dyke emplacement is valid for a given volcanic terrain or magmatic complex is often not straightforward, but it is important for a correct tectonic and geodynamic understanding of that igneous event. It is this issue that we address in this paper with a particular reference to dykes in the Sarnu-Dandali alkaline complex, Rajasthan, northwestern India.

The Sarnu-Dandali complex contains a range of alkaline rock types from mafic (nephelinites, melanephelinites, alkali pyroxenites) to felsic (alkali syenites, phonolites), as well as carbonatites (e.g., Udas et al., 1974; Narayan Das et al., 1978; Srivastava, 1989; Chandrasekaran and Chawade, 1990; Chandrasekaran et al., 1990; Shastry and Kumar, 1996; Simonetti et al., 1998; Bhushan and Chandrasekaran, 2002; Bhushan and Kumar, 2013; Bhushan, 2015). The complex is considered to represent an early alkaline manifestation of the ~65 Ma Deccan flood basalt volcanism based on a single $^{40}Ar/^{39}Ar$ age of 68.57 ± 0.08 Ma (2σ) obtained on an alkali pyroxenite (Basu et al., 1993). The complex is near the northwestern limit of the Deccan province, 500–800 km from the main flood basalt outcrop (Fig. 1a). Here we describe the regional geology and field observations, present geochemical data on the dykes and their host rocks, and discuss the significance of these dykes to the important question of whether it was

* Corresponding author. Tel.: +91 22 25767264; fax: +91 22 25767253.
E-mail address: hcsheth@iitb.ac.in (H. Sheth).
Peer-review under responsibility of China University of Geosciences (Beijing).

http://dx.doi.org/10.1016/j.gsf.2015.09.004

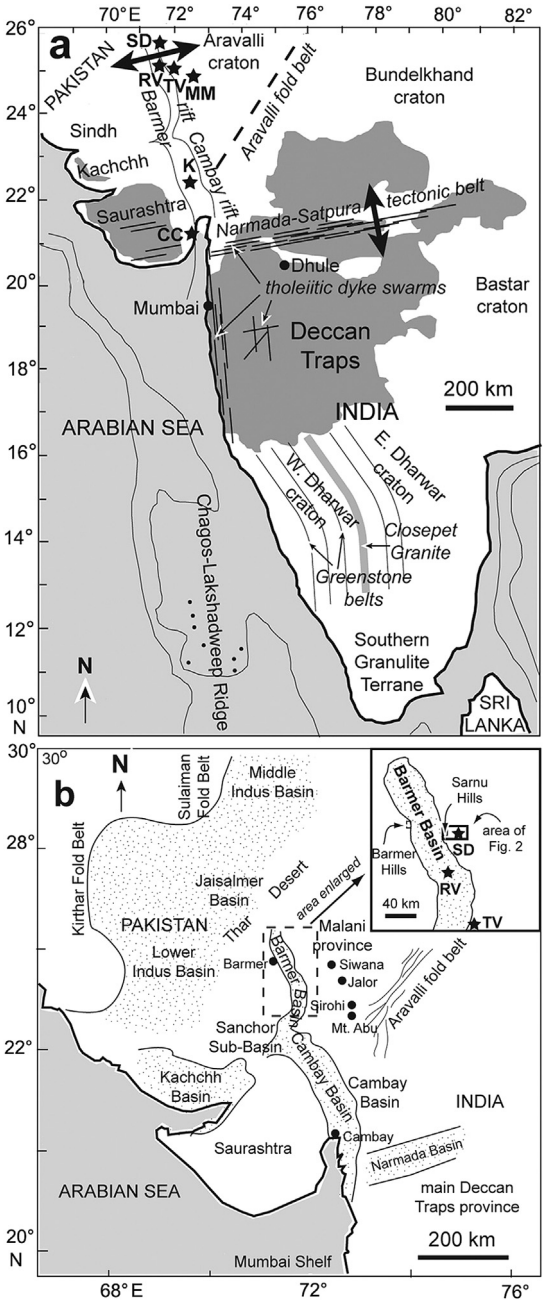

Figure 1. (a) Map of India and the Deccan Traps (modified from Sen et al., 2012) with some volcano-plutonic complexes in the northwestern Deccan region marked (black stars). SD—the Sarnu-Dandali complex, TV—the Tavidar volcanics, RV—the Raageshwari volcanics, MM—the Mer Mundwara complex, K—the Kadi syenite pluton, and CC—the Chogat-Chamardi complex. Three major tholeiitic dyke swarms of the Deccan Traps (Vanderkluysen et al., 2011) are also indicated, and heavy double arrows show the directions of regional extension inferred for the Narmada-Tapi dyke swarm and the Barmer-Cambay rift (see text). The major Archaean cratons are indicated. (b) Map of western and northwestern India and adjoining southern Pakistan, showing the major sedimentary basins and rifts with Mesozoic–Quaternary sedimentary rocks. Some key localities mentioned in the text are marked. Based on Bladon et al. (2015a,b).

contemporaneous regional stresses or basement structural fabric that controlled dyke emplacement.

2. Regional geology

The Sarnu-Dandali complex is located on the eastern shoulder of the Barmer Basin. The Barmer Basin and the Cambay Basin to its south form a major, 600 km long, intracontinental rift, with rich oil and gas reserves (Compton, 2009, Fig. 1a and b). The Cambay rift, containing 1000–3200 m thick Deccan basalts overlain by 3000–5500 m thick Tertiary and Quaternary sediments, indicates major post-Deccan subsidence (e.g., Raju, 1968; Biswas, 1982, 1987). High heat flow and a thinned crust (31–33 km) are known for the Cambay rift (Krishnaswamy, 1981; Ramanathan, 1981; Kaila et al., 1990; Pandey and Negi, 1995). Igneous intrusions such as the Kadi syenite and the Chogat-Chamardi complex (Fig. 1a) occur within the rift or on its shoulders (Auden, 1949; Ramanathan, 1981; Sheth et al., 2011). The pre-Deccan history of the Cambay rift is not well known, owing to the scarcity of drillwells penetrating the thick basalt sequences in the rift. However, Ramanathan (1981) mentioned that a few wells have penetrated the basalts and underlying Mesozoic sedimentary rocks and reached Precambrian basement. Geophysical data on the Cambay rift have been used variably to support a pre-Deccan Mesozoic history and associated sedimentation (Kaila et al., 1990) and to negate it (Tewari et al., 1995).

The Barmer Basin, which initiated as a rift basin during early Cretaceous NW–SE extension, underwent further major rifting during late Cretaceous NE–SW extension, and contains >6 km thick Mesozoic sedimentary rocks (Dolson et al., 2015; Bladon et al., 2015a,b). These pre-rift Jurassic and within-rift early to late Cretaceous sediments overlie volcano-plutonic rocks of the ~750 Ma Malani large igneous province (Bhushan and Chandrasekaran, 2002). A ≥800 m thick, Deccan-age, mafic to felsic volcanic sequence (the Raageshwari Volcanics, Fig. 1a and b) is present in the Barmer Basin at a depth of 3 km (Vermani et al., 2010). These may be stratigraphic equivalents of the 67–65 Ma Tavidar volcanics (Sen et al., 2012) which, like the Sarnu-Dandali complex, are situated on the eastern shoulder of the Barmer rift (Fig. 1a and b). Another alkaline plutonic complex, Mer Mundwara, lies farther east outside the rift basin (Fig. 1a) on Malani-age granite basement. It contains many mafic, ultramafic and syenitic rocks as well as carbonatites (e.g., Viswanathan, 1977; Subrahmanyam and Leelanandam, 1989).

3. Field observations and samples

The Sarnu-Dandali area lies at an elevation of ~100–140 m above sea level, and is mostly flat with an extensive cover of Quaternary sands of the Rajasthan desert (Fig. 2; see this figure for all localities and sample locations). The Malani rhyolites and the early Cretaceous Sarnu Sandstone (outcropping in the Sarnu Hills on the eastern shoulder of the Barmer rift, Fig. 2) form the basement of the complex. The Malani rhyolites are probably represented in a black, moderately porphyritic lava flow (our sample SD01) forming a small mound just north of Kamthai village, a N20°W-striking rhyolite dyke (SD03) cutting that flow, and grey rhyolite lava flows (SD07) forming small hillocks 1.5 km northwest of Kamthai. The Sarnu-Dandali complex also contains lava flows, such as a vesicular trachyandesite flow (SD10) at Sanpa containing abundant ≤1 cm plagioclase glomerocrysts, and an andesitic flow (SD12) exposed near Taku Nadi. A highly porphyritic melanephelinite flow (SD11) is exposed near Sarnu. It is subhorizontal, >20 m thick, and has a lateral extent of ~200 m. It exhibits a colonnade of widely spaced, vertical columnar joints with an overlying entablature zone which is extensively weathered into spheroidal boulders (Fig. 3).

Dykes and small plugs of phonolite outcrop just north of Kamthai, three of which we sampled (the N30°W-striking dyke SD02, and two plugs SD04 and SD05). Bhushan and Kumar (2013) have described a rare-earth-element-rich carbonatite plug from the area 2 km SE of Kamthai (Fig. 2). The plug is traversed by a swarm of phonolite dykes and smaller carbonatite dykes and veins with a

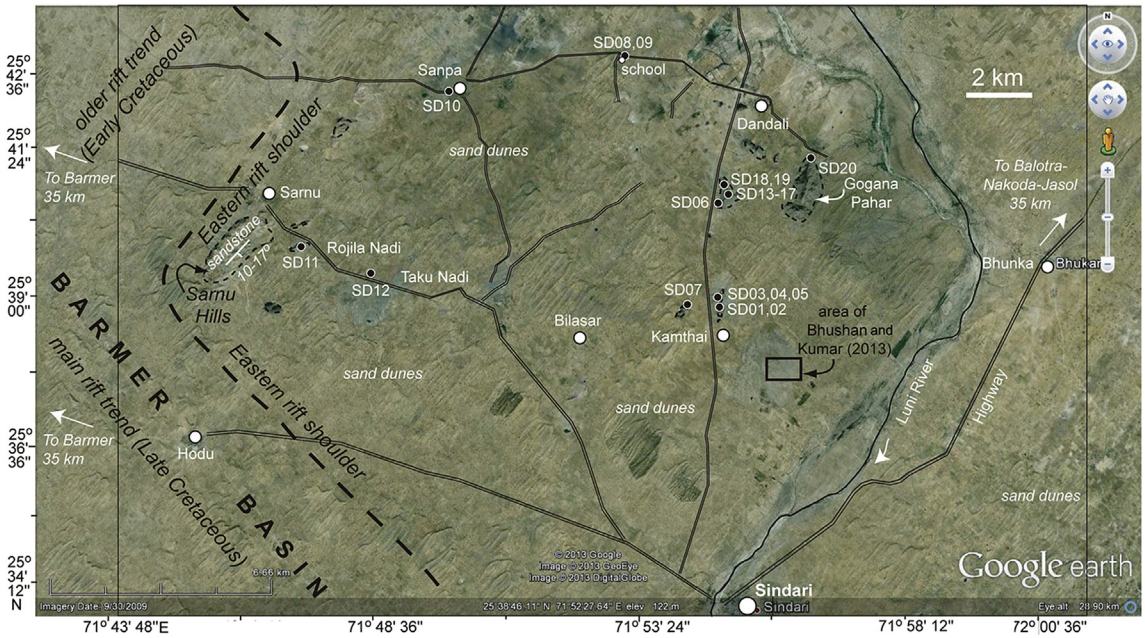

Figure 2. Google Earth image of the study area of the Sarnu-Dandali complex, showing the largely sand-dune-covered, flat landscape and the low hills, with villages, roads (thin double lines) and sample locations (with the prefix SD). Also marked are the study area of Bhushan and Kumar (2013) and the eastern margin of the Barmer Basin (from Bladon et al., 2015a,b).

dominant NNW–SSE trend. Our phonolite dyke SD02 is thus an extension of this swarm. We also collected two more phonolites, representing a plug (SD08) and a N150°-striking, 10 cm wide dykelet (SD09) cutting the plug, halfway between Dandali and Sanpa.

Alkali syenite plutons outcrop 1.5–5 km south of Dandali, and our samples SD06 and SD13 (halfway between Kamthai and Dandali) and SD20 (Gogana Pahar) come from them. The former outcrop is of a coarse-grained (>1 cm) syenite (Fig. 4a) being worked for building stone. It contains mafic enclaves up to tens of centimeters in size, generally rounded and elliptical, and often with gradational margins with the host syenite (Fig. 4b). The syenite pluton is also cut by many dykes, such as nephelinite dykes SD14 (Fig. 4c) and SD18, and phonolite dykes SD15 and SD19 (Fig. 4d), all of which trend NNW–SSE. An exception to this strike direction is

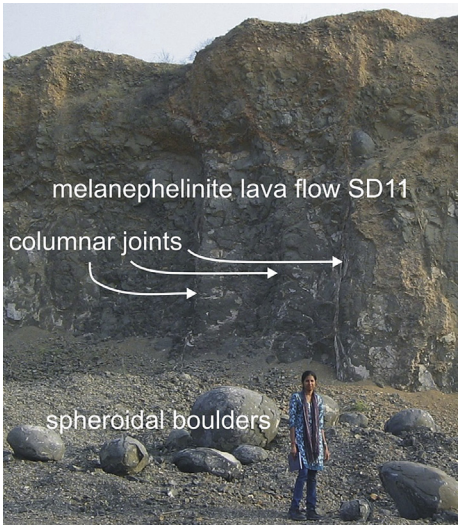

Figure 3. The melanephelinite lava flow SD11 exposed near Sarnu.

Figure 4. Outcrop photographs from the syenite pluton 4 km SSW of Dandali on the road to Kamthai. (a) Close-up view of the syenite SD06. Coin for scale is 2.3 cm in diameter. (b) Several rounded mafic enclaves (en) in the syenite SD13 at the hill summit. This is an oblique view of a horizontal ground surface. (c) 2 m wide nephelinite dyke SD14 intruding the syenite SD13 at the hill summit. (d) Phonolite dyke SD19 cutting the syenite. The background shows the almost flat terrain of the study area's desert landscape. (e) Dyke of peralkaline trachyte SD17 intruding the coarse-grained syenite SD13 with diffuse margins.

provided by a short peralkaline trachyte dyke striking N50°E (SD17, Fig. 4e). Very thin (1–2 cm) and short (tens of cm) veinlets of carbonatite (SD16), with random orientations, also traverse the syenite. Phonolites seem very common in the Sarnu-Dandali complex, comprising 7 of our 20 samples and the longest dykes in the area (up to 800 m, see Fig. 1 of Bhushan and Kumar, 2013).

4. Geochemistry

Rock type identification based on outcrop appearance, hand specimens and even thin sections (in case of very fine-grained or glassy samples) was sometimes difficult. We therefore analyzed 19 samples of Sarnu-Dandali dykes and their host rocks for the major oxides and a few trace elements (Table 1), which enabled us to name the rocks using the total alkali-silica (TAS) diagram (Le Bas et al., 1986, Fig. 5). A discussion of the petrogenesis of these rocks is beyond the scope of this paper and awaits the acquisition of additional trace element and isotopic data.

4.1. Methods

Small, fresh chips of the rocks were cleaned in an ultrasonic bath and ground to powders of <75 μm grain size using a Retsch PM-100 planetary ball mill and stainless steel grinding balls. Then 0.25 g of sample powder was mixed with 0.75 g lithium metaborate ($LiBO_2$) and 0.50 g of lithium tetraborate (LiB_4O_7) in a platinum crucible, and fused in a muffle furnace at 1050 °C for 10 min. After cooling, the crucible was carefully immersed in 80 mL of 1N HCl in a 150-mL glass beaker and then magnetically stirred for 1 h until the fusion bead had dissolved completely. The sample volume was made up to 100 mL in a volumetric flask. Ten mL of this solution diluted to 100 mL with distilled water was analyzed by inductively coupled plasma atomic emission spectrometry (ICPAES) at the Sophisticated Analytical Instrumentation Facility (SAIF), IIT Bombay (instrument: SPECTRO ARCOS) for all major oxides and a few trace elements (Table 1). Several USGS rock standards covering a large compositional range were dissolved along with the samples. The standards DNC-1, BIR-1, BCR-2, AGV-2 and GSP-2 were used for calibrating the instrument, whereas the standards BHVO-2, W-2a and QLO-1 were analyzed as unknowns to estimate the analytical accuracy. Loss on ignition (LOI) values were determined by heating the rock powders at 1000 °C in platinum crucibles, after overnight drying in an oven at 110 °C to drive away adsorbed moisture (H_2O^-).

4.2. Results

The major oxide, LOI and trace element values for the Sarnu-Dandali rocks are presented in Table 1, along with the reference

Table 1
Geochemical data for volcanic and subvolcanic rocks of the Sarnu-Dandali complex, Rajasthan.

Lat.	25°38′53″	25°38′53″	25°38′53″	25°38′56″	25°38′56″	25°40′33″	25°38′54″	25°42′54″	25°42′54″	25°42′20″	25°39′51″	25°39′26″
Long.	71°54′34″	71°54′34″	71°54′34″	71°54′43″	71°54′43″	71°54′43″	71°54′15″	71°53′07″	71°53′07″	71°49′55″	71°47′19″	71°49′02″
Nature	flow	dyke	dyke	pluton	pluton	pluton	flow	pluton	dyke	flow	flow	flow
Trend	–	N150°	N160°	–	–	–		–	N150°	–	–	–
Thickness (cm)		50	30–40						10			
Sample	**SD1**	**SD2**	**SD3**	**SD4**	**SD5**	**SD6**	**SD7**	**SD8**	**SD9**	**SD10**	**SD11**	**SD12**
Rock type	R	PH	R, palk	PH	PH	T, palk	R, palk	PH	PH	TA, lat	FOI, mnp	A
SiO_2	71.72	50.44	74.55	51.14	50.73	63.00	75.78	53.40	57.53	53.75	34.99	56.68
TiO_2	0.44	0.38	0.45	0.35	0.30	0.83	0.39	0.35	0.15	2.07	5.09	1.98
Al_2O_3	10.64	20.86	10.83	21.27	20.58	16.81	9.60	22.94	20.51	15.77	10.44	10.83
$Fe_2O_3^T$	6.97	4.54	6.13	4.66	4.11	3.60	6.28	3.62	3.55	10.43	16.85	11.01
MnO	0.05	0.28	0.03	0.29	0.23	0.12	0.02	0.12	0.27	0.16	0.17	0.11
MgO	0.05	0.22	0.13	0.21	0.20	0.41	0.08	0.32	0.07	2.79	9.92	0.63
CaO	0.89	2.06	0.27	2.04	1.96	1.50	0.54	1.31	0.55	5.25	13.59	14.52
Na_2O	3.12	10.62	6.05	10.64	11.45	7.21	2.89	7.52	11.01	4.57	2.64	0.17
K_2O	4.82	6.61	3.02	6.41	5.40	4.72	4.89	8.96	4.68	2.80	2.09	0.01
P_2O_5	0.06	0.03	0.07	0.04	0.05	0.14	0.01	0.01	0.02	0.44	0.73	0.32
LOI	1.71	3.58	0.73	2.65	4.47	1.28	0.97	2.64	1.17	1.73	2.17	2.84
Total	100.47	99.63	102.25	99.71	99.48	99.62	101.45	101.18	99.50	99.76	98.68	99.09
$Mg^{\#}$	2.02	12.4	5.59	11.6	12.4	24.6	3.53	20.0	5.34	41.9	–	30.95
Q	32.05	–	29.13	–	–	0.14	37.57	–	–	0.92	–	30.95
Or	28.98	40.81	17.63	39.13	33.71	28.45	28.88	53.87	28.17	17.00	–	–
Ab	26.87	1.41	38.50	3.79	10.58	61.37	22.13	2.89	37.23	39.76	–	1.51
An	0.80	–	–	–	–	–	–	2.41	–	14.65	11.00	30.17
Lc	–	–	–	–	–	–	–	–	–	–	10.19	–
Ne	–	39.12	–	39.24	37.60	–	–	33.51	23.71	–	12.72	–
Ac	–	4.26	5.44	4.32	3.89	0.73	2.04	–	3.25	–	–	–
Di	2.95	9.17	0.77	8.95	8.67	5.65	2.31	3.56	2.38	7.63	15.60	28.63
Hy	4.17	–	6.13	–	–	0.44	4.51	–	–	10.84	–	–
Ol	–	0.81	–	1.00	0.65	–	–	1.41	2.54	–	23.58	–
Mt	3.19	–	–	–	–	1.29	1.80	1.65	–	4.11	3.92	4.01
Il	0.86	0.76	0.85	0.69	0.60	1.61	0.74	0.67	0.29	4.05	10.17	3.95
Ap	0.13	0.08	0.16	0.10	0.13	0.32	0.03	0.02	0.04	1.04	1.78	0.79
Ns	–	3.58	1.39	2.78	4.16	–	–	–	2.40	–	–	–
Cs	–	–	–	–	–	–	–	–	–	–	11.04	–
Sc	0.38	bdl	4.39	bdl	bdl	1.60	bdl	bdl	bdl	12.0	37.8	24.1
Co	3.90	3.66	3.25	2.92	3.50	5.21	2.88	2.40	0.28	26.9	74.0	21.5
Ni	40.0	6.30	19.1	6.88	6.06	10.4	22.9	10.1	9.95	8.47	108	38.2
Sr	28.5	1808	55.9	1779	1904	149	29.8	1707	183	497	930	1953
Zr	1165	498	1383	547	598	577	1404	425	2217	472	282	133
Ba	72.5	3308	67.0	2798	1367	1348	71.9	2675	107	545	835	15.4

Lat.	25°40′47″	25°40′47″	25°40′47″	25°40′47″	25°40′49″	25°40′49″	25°41′20″				
Long.	71°54′54″	71°54′54″	71°54′54″	71°54′54″	71°54′52″	71°54′52″	71°56′32″				
Nature	pluton	dyke	dyke	dyke	dyke	dyke	pluton				
Trend	–	N320°	N330°	N50°	N330°	N345°	–				
Thickness (cm)		200	90	10–15	20	40–45					
Sample	**SD13**	**SD14**	**SD15**	**SD17**	**SD18**	**SD19**	**SD20**	**W-2a**	**W-2a**	**BHVO2**	**BHVO2**
Rock type	T, palk	FOI, np	PH	T, palk	FOI, np	PH	T	Ref.	Meas.	Ref.	Meas.
SiO_2	63.65	43.24	47.82	63.53	42.18	50.94	61.72	52.68	52.71	49.9	50.83
TiO_2	0.60	1.76	0.62	0.85	1.13	0.41	0.77	1.06	1.09	2.73	2.82
Al_2O_3	16.89	18.79	20.48	16.76	17.74	20.43	16.65	15.45	15.08	13.5	13.68
$Fe_2O_3^T$	3.84	8.84	6.12	3.53	8.35	3.98	3.57	10.83	11.74	12.3	13.55
MnO	0.14	0.29	0.21	0.18	0.37	0.19	0.23	0.167	0.12	0.166	0.17
MgO	0.53	1.66	0.46	0.49	1.20	0.32	0.50	6.37	6.69	7.23	7.59
CaO	1.00	6.67	3.04	0.93	6.87	1.90	2.72	10.86	10.84	11.4	11.56
Na_2O	7.52	10.13	11.09	7.74	9.28	11.31	7.07	2.20	2.23	2.22	2.21
K_2O	4.85	4.47	5.79	5.12	4.38	4.70	4.55	0.626	0.49	0.52	0.46
P_2O_5	0.14	0.41	0.08	0.06	0.22	0.09	0.14	0.14	0.12	0.27	0.28
LOI	0.74	1.61	2.35	0.95	8.05	4.56	2.23				
Total	99.88	97.86	98.06	100.14	99.76	98.84	100.15	100.38	101.11	100.24	103.15
$Mg^{\#}$	28.28	33.53	17.79	28.62	27.87	18.59	28.58				
Q	–	–	–	–	–	–	–				
Or	28.99	–	25.54	30.59	–	29.57	27.55				
Ab	59.85	–	–	57.69	–	17.38	58.15				
An	–	–	–	–	–	–	0.26				
Lc	–	21.67	8.14	–	22.26	–	–				
Ne	0.39	40.67	41.54	0.34	39.76	36.05	1.68				
Ac	3.33	7.08	5.77	3.20	7.02	3.80	–				
Di	3.51	19.38	13.31	3.66	23.54	8.15	8.88				
Hy	–	–	–	–	–	–	–				
Ol	2.39	2.42	0.71	1.77	0.78	0.83	–				
Mt	0.08	–	–	–	–	–	1.64				
Il	1.14	3.50	1.24	1.63	2.36	0.83	1.49				
Ap	0.32	0.99	0.18	0.13	0.56	0.23	0.34				
Ns	–	1.52	3.55	0.98	1.13	3.15	–				
Cs	–	2.76	–	–	2.60	–	–				
Sc	1.88	1.54	0.02	0.71	bdl	bdl	1.92	36	36.9	32	33.0
Co	4.27	18.7	7.22	6.20	13.2	2.23	4.91	43	35.7	45	47.4
Ni	8.25	4.55	3.96	8.31	1.44	3.81	8.77	70	71.4	119	120
Sr	180	2252	1724	133	2785	983	176	190	196	389	409
Zr	606	426	423	590	513	669	152	100	91.8	172	170
Ba	800	1203	1971	470	1721	1283	1586	170	174	130	140

Notes: Major oxides are in wt.% and the trace elements in parts per million (ppm). $Fe_2O_3^T$ is total iron expressed as Fe_2O_3. Abbreviated mineral names in italics are CIPW normative minerals (in wt.%) as computed by the SINCLAS program of Verma et al. (2002), based on LOI-free recalculated data and the Middlemost (1989) scheme of division of total iron into Fe^{2+} and Fe^{3+} categories. *Ns* is sodium metasilicate and *Cs* calcium silicate. Rock types (names) are also as determined by SINCLAS based on the total alkali-silica diagram of Le Bas et al. (1986) and the abbreviations are: R (rhyolite), PH (phonolite), T (trachyte), TA (trachyandesite), lat (latite), A (andesite), FOI (foidite), np (nephelinite), mnp (melanephelinite). The qualifier "palk" means a peralkaline (syn. agpaitic) character. "bdl" indicates concentration below detection limit. All analyzed samples are silicate rocks; an associated carbonatite dyke sample SD16 (N 25°40′47″, E 71°54′54″) was not analyzed. Reference and measured values on the USGS standards W-2a and BHVO2 (Wilson, 2000 and Wilson, crustal.usgs.gov/geochemical_reference_standards/powdered_RM.html) provide an idea about analytical accuracy.

and measured values on USGS standards. CIPW norms for all samples computed using the SINCLAS program of Verma et al. (2002) are also presented in Table 1.

The high analytical accuracy of the analyses is indicated by the very close reference and measured values on the standards. Almost all analyses have major oxide and LOI totals that are very close to 100 wt.%. The major and trace element concentrations measured in the different rock types also closely match those reported for the same rock types by Chandrasekaran et al. (1990), Simonetti et al. (1998), and Bhushan and Chandrasekaran (2002). For example, we find Na_2O in our syenites and phonolites to be greater or much greater than K_2O. The phonolites have 23–41 wt.% normative nepheline, and the melanephelinite SD11 has 12.72 wt.% normative nepheline and 23.58 wt.% normative olivine. The syenites SD06, SD13 and SD20 are classified by SINCLAS as trachyte, the former two peralkaline. As required of peralkaline rocks (e.g., Currie, 1989; Best, 2003, p. 707; Winter, 2011, p. 152), these samples have agpaitic index [the molar $(Na_2O + K_2O)/Al_2O_3$ ratio] ≥ 1, they contain alkali-rich mafic minerals and normative acmite, and lack normative anorthite. Srivastava (1989) also noted that the Sarnu-Dandali syenites were "agpaitic", with normative acmite.

Whereas all our rocks are alkaline *sensu stricto* (Fig. 5; cf. Bhushan and Chandrasekaran, 2002), the andesite SD12 is subalkaline. Noting its unusually low alkalis and moderately high LOI value, we suspect that weathering may have caused loss of alkalis from it. We note that a few samples of Chandrasekaran et al. (1990) are also subalkaline. Several of our phonolites have very high total alkali values ($\geq$17 wt.%), and such values are also found in the samples of Simonetti et al. (1998) and Bhushan and Chandrasekaran (2002, Fig. 5).

5. Discussion

5.1. Early synplutonic dykes vs. the coherent dykes

Mingling of co-existing mafic and felsic magmas is indicated by the abundant mafic enclaves in the syenite pluton (SD06, SD13) 4 km south of Dandali. The enclaves (described as alkali olivine basalt by Bhushan and Chandrasekaran, 2002) indicate that the two magmas did not mix and hybridize completely because of their composition, temperature and viscosity contrast (e.g., Snyder, 2000; Zellmer et al., 2012; Jayananda et al., 2014). The enclaves

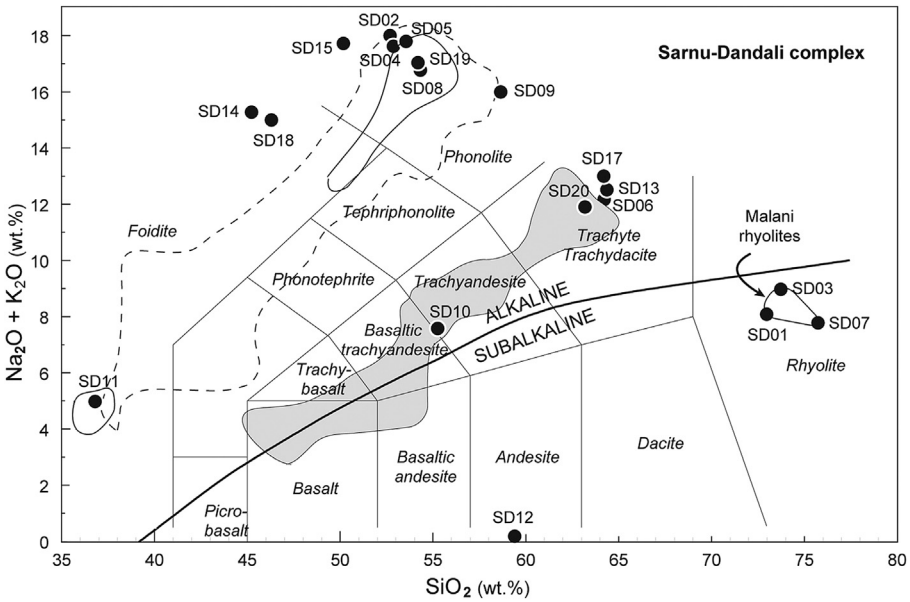

Figure 5. Data for the Sarnu-Dandali rocks of this study (filled circles) plotted on the total alkali-silica (TAS) diagram (Le Bas et al., 1986). Boundary line between the subalkalic and alkalic fields is after Irvine and Baragar (1971). Samples SD01, SD03 and SD07 probably represent the Malani rhyolites (see text). Fields are also shown for Sarnu-Dandali data of previous workers, namely Chandrasekaran et al. (1990, shaded field), Simonetti et al. (1998, two fields with continuous boundaries), and Bhushan and Chandrasekaran (2002, field with discontinuous boundary). All data are adjusted to 100% on an LOI-free basis using the SINCLAS program (Verma et al., 2002).

could have formed by the disaggregation of one or more mafic "synplutonic" dykes which entered the syenite pluton when it was still largely liquid (e.g., Jayananda et al., 2009). On the other hand, the coherent dykes in the same syenite pluton, such as the nepheline SD14 and the phonolite SD19 (Fig. 4c and d), represent magma-driven fracture propagation in the same syenite when it was essentially solid. The orientations of the early synplutonic dykes are unknown, but those of the coherent dykes can be determined, and give valuable information on the question at hand.

5.2. Consistency of dyke strike directions

Of the dykes sampled, four dykes (the phonolites SD02, SD09 and SD15, and the nephelinite SD18) strike N30°W, the rhyolite SD03 strikes N20°W, the nephelinite SD14 strikes N40°W, and the phonolite SD19 strikes N15°W. They have near-vertical or very steep dips. Seven of these dykes thus strike ~NNW–SSE, and this is irrespective of dyke thickness which varies from 1–2 cm to 2 m (Table 1; Fig. 6a). One dyke (peralkaline trachyte SD17) strikes N50°E, and we observed (but did not sample) additional dykes with NNW–SSE strike (e.g., north of Kamthai).

From the area 2 km SE of Kamthai (Fig. 2), Bhushan and Kumar (2013) showed numerous phonolite dykes up to 800 m in length (with their lateral ends covered by desert sand), carbonatite dykes up to 200 m long, and carbonatite veins. A dominance of the NNW–SSE strike is obvious from their map, which shows eight phonolite dykes >300 m long, with slightly curved trace, and a general strike direction of N20°W (Fig. 6a). We thus estimate that >95% of the dykes in the Sarnu-Dandali complex trend NNW–SSE, and we discuss the significance of this result below.

5.3. Tectonic significance of the dyke trends

Undeformed dykes are very useful palaeostress indicators, because most dykes propagate as magma-driven extension fractures (mode I cracks) akin to hydraulic fractures that form perpendicular to the minimum principal compressive stress σ_3 (e.g., Pollard, 1987; Gudmundsson and Marinoni, 2002; Tibaldi, 2015). The maximum (σ_1) and intermediate (σ_2) principal compressive stress directions lie normal to one another within the plane of the dyke. The dominantly NNW–SSE strike direction of the Sarnu-Dandali dykes suggests that the regional minimum principal compressive stress (or the maximum tensile stress, σ_3) was aligned ENE–WSW during dyke emplacement. The small spread observed in dyke strike directions may reflect local or transient fluctuations in the σ_3 direction about a time-averaged NNW–SSE mean direction (e.g., Gudmundsson, 1995; Ray et al., 2007). In any given swarm, the regional dykes more accurately reflect the prevalent regional stress directions, whereas smaller dykes show a larger dispersion from the swarm's mean direction (e.g., Babiker and Gudmundsson, 2004; Ray et al., 2007). Thus the phonolite dykes up to 800 m long and consistently N20°W-trending (Bhushan and Kumar, 2013) indicate a regional ENE–WSW extension.

The small peralkaline dyke SD17 which strikes N50°E may be related to a temporary switch in the principal stress directions following intensive dyking along the NNW–SSE direction (Babiker and Gudmundsson, 2004; Ray et al., 2007). Note that its N50°E trend has nothing to do with the early Cretaceous NW–SE σ_3 direction inferred from the Sarnu Sandstone (Bladon et al., 2015a,b) and the dyke is altogether later, like its host syenite. The randomly oriented carbonatite veinlets probably occupy cooling joints in the syenite pluton.

5.4. Dyke and rift trends: passive inheritance of older structural fabric?

The question of whether regional swarms of preferentially oriented dykes form during contemporaneous regional extension, or whether they simply exploit pre-existing lines of weakness or structural fabric in their basement rocks, has been debated, and arguments exist for both mechanisms in specific case studies (Delaney et al., 1986; Baer et al., 1994; Delaney and Gartner, 1997; Mège and Korme, 2004; Ray et al., 2007; Tibaldi, 2015). Dykes of highly irregular shapes, with considerable internal variations in

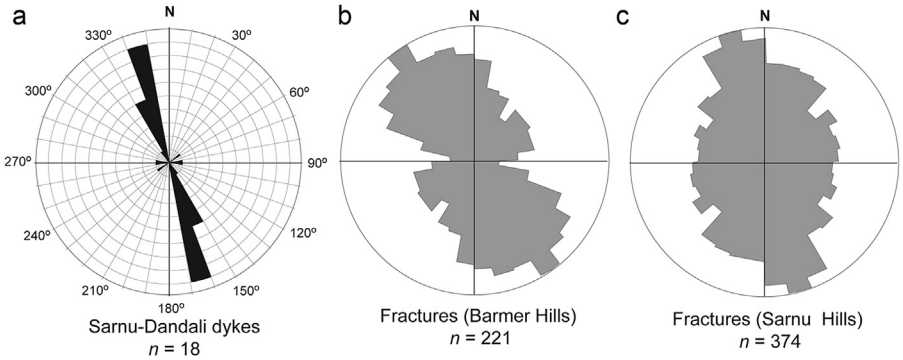

Figure 6. (a) Rose diagram of the Sarnu-Dandali dyke strike directions, with data from the present study and Bhushan and Kumar (2013). Data are only for silicate rock dykes. Data for many small and highly randomly oriented carbonatite dykes shown in Bhushan and Kumar (2013) are not plotted. (b, c) Rose diagrams of fractures cutting Malani rocks and Palaeocene sedimentary rocks in the Barmer Hills, and fractures in the Sarnu Sandstone in the Sarnu Hills (based on Bladon et al., 2015a). Note the dominance of the NNW–SSE trend in all plots.

strike and dip directions and thickness, have been argued to follow the fracture sets in their basement rocks rather than the regional stress field (Baer et al., 1994). However, classical tabular or planar dykes could also be following basement fabric. We evaluate the possibility that the consistently NNW–SSE trends of the Sarnu-Dandali dykes are related to basement fabric.

There is no question that the Sarnu-Dandali dykes are parallel to the NNW–SSE trend of the Barmer-Cambay rift. The Indian rift zones have been hypothesized to have developed along Precambrian structural trends (e.g., Naqvi et al., 1974; Katz, 1979; Naqvi and Rogers, 1987). In particular, the Barmer-Cambay rift and the western Indian rifted continental margin have been hypothesized to have developed along the Dharwar structural trend of the southern Indian shield (Fig. 1a; Raju, 1968; Biswas, 1982, 1987; Gombos et al., 1995). If so, the Sarnu-Dandali dykes could also reflect the control of this ancient structural trend. However, there are problems with this scenario. For one, we ask *what* is the Dharwar trend. The strike direction of the Dharwar greenstone belts, as well as the 2.5 Ga Closepet Granite bounding the western Dharwar and the eastern Dharwar cratons, changes from N–S in the southern part to NNW–SSE in the northern part, over a 500 km strike distance (see the geological maps in Senthil Kumar et al., 2007 and Jayananda et al., 2009, 2014, for example). It is highly unlikely that the same NNW–SSE strike continues northward undeflected, for an additional 1000 km, reaching western Rajasthan.

Secondly and more importantly, the hypothesized control of the Dharwar structural trend on the Barmer-Cambay rift orientation *requires* that the Dharwar craton be present under western Rajasthan. Though the Dharwar craton extends under the Deccan basalt cover to the Dhule area (Fig. 1a; Senthil Kumar et al., 2007; Ray et al., 2008; Upadhyay et al., 2015), its extension further north is unknown. Its presence beneath the Barmer rift is highly unlikely, and impossible if the Narmada-Satpura tectonic belt represents a Proterozoic protocontinental suture between a northern (Aravalli) protocontinent and a southern (Dharwar) protocontinent (Naqvi et al., 1974). We therefore think that the hypothesized control of the "Dharwar trend" on the Barmer-Cambay rift (Raju, 1968; Biswas, 1982, 1987; Gombos et al., 1995) is speculative and unfounded. We now consider the possible basement trends under the Barmer rift, present in the Aravalli craton. These may be the NE–SW trend of the Proterozoic Aravalli fold belt (Fig. 1a and b) or the NNE–SSW trend of the Malani volcanic sequences (Roy, 2001; Sharma, 2004, 2005). The Barmer-Cambay rift and the Sarnu-Dandali dykes clearly do not follow these Precambrian trends.

How about the early Cretaceous fractures and normal faults identified in the Barmer rift? Bladon et al. (2015a,b) stated that the Barmer rift formed during two distinct episodes of crustal extension. The first was in the early Cretaceous with NW–SE extension, related to the separation of West Gondwana from East Gondwana. The Barmer rift developed as isolated, NE–SW-trending basins and the Sarnu Sandstone, containing abundant NE–SW fractures and extensional faults, was deposited during this time. The late Cretaceous, overwhelmingly NNW–SSE-trending Sarnu-Dandali dykes did not passively occupy the early Cretaceous NE–SW structural fabric of the Sarnu Sandstone, which outcrops adjacent to the complex (Fig. 2).

This discussion shows that the Sarnu-Dandali dyke trends or the Barmer-Cambay rift orientations were not controlled by Precambrian basement structure, and the dyke trends were also not controlled by pre-existing, early Cretaceous extensional structures in the uppermost crust.

5.5. Dyke and rift trends: contemporaneous, late Cretaceous regional extension

If the trends of the Sarnu-Dandali dykes and the Barmer-Cambay rift were not controlled by basement structure, they must reflect contemporaneous regional stress fields. Bladon et al. (2015a,b) found that the Barmer rift acquired its present size and overall NNW–SSE trend during its second, major extensional episode in the late Cretaceous. This episode involved NE–SW extension. It produced NW–SE-directed fractures and normal faults in the Malani and Palaeocene sedimentary rocks exposed in the Barmer Hills on the western rift shoulder (Fig. 6b), and also in the early Cretaceous Sarnu Sandstone on the eastern rift shoulder (Fig. 6c).

There is independent geological evidence for NE–SW-directed late Cretaceous regional extension in western-northwestern India which eventually led to the rifting of the Seychelles microcontinent from India at ~62 Ma (Collier et al., 2008). This pre-breakup NE–SW regional extension is reflected in the formation of several rift basins in western and northwestern Rajasthan (Sharma, 2007) and is supported by recent plate motion reconstructions (Reeves, 2014) and structural mapping results indicating oblique and strike-slip movements (Misra et al., 2014). Bladon et al. (2015a,b) argued that the present 600 km long Barmer-Cambay rift was formed in the late Cretaceous due to far-field stresses caused by these ongoing plate reorganizations (see also Sharma, 2007). We therefore suggest that the abundant NW–SE fractures in the Barmer rift sediments, the NNW–SSE-striking Sarnu-Dandali dykes

and the much larger-scale Barmer-Cambay rift were all produced in a single tectonic regime of regional NE–SW extension in late Cretaceous–Palaeocene time.

From the NNW–SSE-trending Sarnu-Dandali dykes and the Barmer-Cambay rift, we infer a ENE–WSW late Cretaceous regional σ_3 direction (see heavy double arrows in Fig. 1b). Interestingly, strongly ENE–WSW-trending tholeiitic dyke swarms in the Narmada-Satpura tectonic zone (Ray et al., 2007; Sheth et al., 2011; Vanderkluysen et al., 2011; Ju et al., 2013) imply a NNW–SSE late Cretaceous regional σ_3 direction (Fig. 1b). These two regional extension directions would have summed to generate overall NE–SW extension in the region between the Narmada-Satpura tectonic zone and the Barmer-Cambay rift, explaining the eventual NE–SW-directed separation of the Seychelles from India.

6. Conclusions

This case study contributes useful data to the important but sometimes difficult question of whether oriented dyke swarms reflect contemporaneous regional stresses or basement fabric. The Sarnu-Dandali alkaline complex is located on the eastern shoulder of the 600 km long Barmer-Cambay rift, which is known to have formed in the early Cretaceous, with later major rifting, subsidence and sedimentation from the late Cretaceous onwards (Bladon et al., 2015a,b; Dolson et al., 2015). Imprints of the early Cretaceous NW–SE-directed extensional deformation are preserved on the eastern rift shoulder in NE–SW-trending extensional fractures and normal faults in the Sarnu Sandstone. Yet almost none of the compositionally varied and dominantly NNW–SSE-trending dykes in the spatially adjacent, late Cretaceous Sarnu-Dandali complex have this strike direction, or the trends of the Aravalli fold belt (NE–SW) or the Malani igneous suite (NNE–SSW). It is impossible that the dykes or the Barmer-Cambay rift were controlled by the Precambrian Dharwar trend of the southern Indian shield. Therefore, these small and large structures did not passively exploit pre-existing structural fabric in their basement rocks. The late Cretaceous NW–SE-trending extensional fractures and faults seen in the Barmer and Sarnu Hills, and the NNW–SSE-trending Sarnu-Dandali dykes and the much larger-scale Barmer-Cambay rift were all formed due to contemporaneous, regional ENE–WSW extension, for which there is ample independent geological evidence.

Acknowledgments

Field work was supported by the Industrial Research and Consultancy Centre (IRCC), IIT Bombay (Grant No. 09YIA001 to Sheth). Vijayan has been supported by a Ph.D. Scholarship from the University Grants Commission (UGC), Govt. of India. We thank Reshma Shinde and Laiq S. Mombasawala for valuable help with the ICPAES analyses at SAIF, IIT Bombay. We thank Stuart Burley for supplying several papers and for helpful e-mail discussions. T. K. Biswal, K. Pande, G. Mathew and S. G. Viladkar are thanked for valuable discussions, and Alessandro Tibaldi, Gerhard Wörner, Christoph Breitkreuz and Ciro Cucciniello for critical comments on an earlier version of this work. The present manuscript became significantly revised, focused and improved by the critical journal reviews of P. Senthil Kumar and an anonymous referee, as well as Associate Editor E. Shaji.

References

Auden, J.B., 1949. Dykes in western India – a discussion of their relationships with the Traps, Deccan Traps. Transactions of the National Academy of Sciences (India) 3, 123–157.

Babiker, M., Gudmundsson, A., 2004. Geometry, structure and emplacement of mafic dykes in the Red Sea Hills, Sudan. Journal of African Earth Sciences 38, 279–292.

Baer, G., Beyth, M., Reches, Z., 1994. Dykes emplaced into fractured basement, Timna igneous complex, Israel. Journal of Geophysical Research 99, 24039–24050.

Le Bas, M.J., Le Maitre, R.W., Streckeisen, A., Zanettin, P., 1986. A chemical classification of volcanic rocks based on the total alkali-silica diagram. Journal of Petrology 27, 745–750.

Basu, A.R., Renne, P.R., Das Gupta, D.K., Teichmann, F., Poreda, R.J., 1993. Early and late alkali pulses and a high ^{3}He plume origin for the Deccan flood basalts. Science 261, 902–906.

Best, M.G., 2003. Igneous and Metamorphic Petrology, second ed. Blackwell Publishing. 729 pp.

Bhushan, S.K., 2015. Geology of the Kamthai rare earth deposit. Journal of Geological Society of India 85, 537–546.

Bhushan, S.K., Chandrasekaran, V., 2002. Geology and geochemistry of the magmatic rocks of the Malani igneous suite and tertiary alkaline province of western Rajasthan, vol. 126. Geological Survey of India Memoir, 179 pp.

Bhushan, S.K., Kumar, A., 2013. First carbonatite hosted REE deposit from India. Journal of Geological Society of India 81, 41–60.

Biswas, S.K., 1982. Rift basins in western margins of India and their hydrocarbon prospects with special reference to Kutch basin. American Association of Petroleum Geologists Bulletin 66, 1497–1513.

Biswas, S.K., 1987. Regional tectonic framework, structure and evolution of western marginal basins of India. Tectonophysics 135, 305–327.

Bladon, A.J., Clarke, S.M., Burley, S.D., 2015a. Complex rift geometries resulting from inheritance of pre-existing structures: insights and regional implications from the Barmer Basin rift. Journal of Structural Geology 71, 136–154.

Bladon, A.J., Burley, S.D., Clarke, S.M., Beaumont, H., 2015b. Geology and regional significance of the Sarnoo Hills, eastern rift margin of the Barmer Basin, NW India. Basin Research 27 (5), 636–655.

Chandrasekaran, V., Chawade, M.P., 1990. Carbonatites of the Barmer District, Rajasthan. Indian Minerals 44, 315–324.

Chandrasekaran, V., Srivastava, R.K., Chawade, M.P., 1990. Geochemistry of the alkaline rocks of Sarnu-Dandali area, District Barmer, Rajasthan, India. Journal of Geological Society of India 36, 365–382.

Collier, J.S., Sansom, V., Ishizuka, O., Raylor, R.N., Minshull, T.A., Whitmarsh, R.B., 2008. Age of Seychelles-India breakup. Earth and Planetary Science Letters 272, 264–277.

Compton, P.M., 2009. The geology of the Barmer Basin, Rajasthan, India, and the origins of its major oil reservoir, the Fatehgarh Formation. Petroleum Geoscience 15, 117–130.

Currie, K.L., 1989. New ideas on an old problem: the peralkaline rocks. In: Leelanandam, C. (Ed.), Alkaline Rocks. Geological Society of India Memoir, vol. 15, pp. 117–136.

Delaney, P.T., Gartner, A.E., 1997. Physical processes of shallow mafic dyke emplacement near the San Rafael swell, Utah. Geological Society of America Bulletin 109, 1177–1192.

Delaney, P.T., Pollard, D.D., Ziony, J.I., McKee, E.H., 1986. Field relations between dykes and joints: emplacement processes and palaeostress analysis. Journal of Geophysical Research 91, 4920–4938.

Dolson, J., Burley, S.D., Sunder, V.R., Kothari, V., Naidu, B., Whiteley, N.P., Farrimond, P., Taylor, A., Direen, N., Ananthakrishnan, B., 2015. The discovery of the Barmer Basin, Rajasthan, India, and its petroleum geology. American Association of Petroleum Geologists Bulletin 99, 433–465.

Gombos, A.M., Powell, W.G., Norton, I.O., 1995. The tectonic evolution of western India and its impact on hydrocarbon occurrences: an overview. Sedimentary Geology 96, 119–129.

Gudmundsson, A., 1995. Infrastructure and mechanics of volcanic systems in Iceland. Journal of Volcanology and Geothermal Research 64, 1–22.

Gudmundsson, A., Marinoni, L.B., 2002. Geometry, emplacement, and arrest of dykes. Annales Tectonicae 13, 71–92.

Irvine, T.N., Baragar, W.R.A., 1971. A guide to the chemical classification of the common rocks. Canadian Journal of Earth Sciences 8, 523–548.

Jayananda, M., Miyazaki, T., Gireesh, R.V., Mahesha, N., Kano, T., 2009. Synplutonic mafic dykes from Late Archaean granitoids in the Eastern Dharwar Craton, southern India. Journal of Geological Society of India 73, 117–130.

Jayananda, M., Gireesh, R.V., Sekhamo, K.-U., Miyazaki, T., 2014. Coeval felsic and mafic magmas in Neoarchean calc-alkaline magmatic arcs, Dharwar craton, southern India: field and petrographic evidence from mafic to hybrid magmatic enclaves and synplutonic mafic dykes. Journal of Geological Society of India 84, 5–28.

Ju, W., Hou, G., Hari, K., 2013. Mechanics of mafic dyke swarms in the Deccan large igneous province: palaeostress field modelling. Journal of Geodynamics 66, 79–91.

Kaila, K.L., Tewari, H.C., Krishna, V.G., Dixit, M.M., Sarkar, D., Reddy, M.S., 1990. Deep seismic sounding studies in the north Cambay and Sanchor basins, India. Geophysical Journal International 103, 621–637.

Katz, M.B., 1979. India and Madagascar in Gondwanaland based on matching Precambrian lineament. Nature 279, 312–315.

Krishnaswamy, V.S., 1981. The Deccan volcanic episode, related tectonism and geothermal manifestations. In: Subbarao, K.V., Sukheswala, R.N. (Eds.), Deccan Volcanism. Geological Society of India Memoir, vol. 3, pp. 1–7.

Mège, D., Korme, T., 2004. Dyke swarm emplacement in the Ethiopian large igneous province: not only a matter of stress. Journal of Volcanology and Geothermal Research 132, 283–310.
Middlemost, E.A.K., 1989. Iron oxidation ratios, norms and the classification of volcanic rocks. Chemical Geology 77, 19–26.
Misra, A.A., Bhattacharya, G., Mukherjee, S., Bose, N., 2014. Near N-S palaeo-extension in the western Deccan region, India: does it link strike-slip tectonics with India-Seychelles rifting? International Journal of Earth Sciences 103, 1645–1680.
Naqvi, S.M., Rao, V.D., Narain, H., 1974. The protocontinental growth of the Indian shield and the antiquity of its rift valleys. Precambrian Research 1, 345–398.
Naqvi, S.M., Rogers, J.J.W., 1987. Precambrian Geology of India. Clarendon Press, New York, p. 238.
Narayan Das, G.R., Bagchi, A.K., Chaube, D.N., Sharma, C.V., Navaneethan, V., 1978. Rare metal contents, geology and tectonic setting of the alkaline complexes across the trans-Aravalli region, Rajasthan. Recent Researches in Geology 7, 201–219.
Pandey, O.P., Negi, J.G., 1995. Geothermal fields of India: a latest update. Proceedings of the World Geothermal Congress (Florence) 1, 163–172.
Pollard, D.D., 1987. Elementary fractures mechanics applied to the structural interpretation of dykes. In: Halls, H.C., Fahrig, W.H. (Eds.), Mafic Dyke Swarms. Geological Association of Canada Special Paper, vol. 34, pp. 5–24.
Raju, A.T.R., 1968. Geological evolution of Assam and Cambay tertiary basins of India. American Association of Petroleum Geologists Bulletin 52, 2422–2437.
Ramanathan, S., 1981. Some aspects of Deccan volcanism of western Indian shelf and Cambay Basin. In: Subbarao, K.V., Sukheswala, R.N. (Eds.), Deccan Volcanism. Geological Society of India Memoir, vol. 3, pp. 198–217.
Ray, R., Sheth, H.C., Mallik, J., 2007. Structure and emplacement of the Narmada-Dhule mafic dyke swarm, Deccan Traps, and the tectonomagmatic evolution of flood basalts. Bulletin of Volcanology 69, 537–551.
Ray, R., Shukla, A.D., Sheth, H.C., Ray, J.S., Duraiswami, R.A., Vanderkluysen, L., Rautela, C.S., Mallik, J., 2008. Highly heterogeneous Precambrian basement under the central Deccan Traps, India: direct evidence from xenoliths in dykes. Gondwana Research 13, 375–385.
Reeves, C., 2014. The position of Madagascar within Gondwana and its movements during Gondwana dispersal. Journal of African Earth Sciences 94, 45–57.
Roy, A.B., 2001. Neoproterozoic crustal evolution of northwestern Indian shield: implications on break up and assembly of supercontinents. Gondwana Research 4, 289–306.
Sen, A., Pande, K., Hegner, E., Sharma, K.K., Dayal, A.M., Sheth, H.C., Mistry, H., 2012. Deccan volcanism in Rajasthan: ^{40}Ar-^{39}Ar geochronology and geochemistry of the Tavidar volcanic suite. Journal of Asian Earth Sciences 59, 127–140.
Senthil Kumar, P., Menon, R., Koti Reddy, G., 2007. Crustal geotherm in the southern Deccan basalt province, India: the Moho is as cold as surrounding cratons. In: Foulger, G.R., Jurdy, D.M. (Eds.), Plates, Plumes, and Planetary Processes. Geological Society of America Special Paper, vol. 430, pp. 275–284.
Sharma, K.K., 2004. The Neoproterozoic Malani magmatism of the northwestern Indian shield: implications for crust-building processes. In: Sheth, H.C., Pande, K. (Eds.), Magmatism in India through Time. Proceedings of the Indian Academy of Sciences (Earth and Planetary Sciences), vol. 113, pp. 795–807.
Sharma, K.K., 2005. Malani magmatism: an extensional lithospheric tectonic origin. In: Foulger, G.R., Natland, J.H., Presnall, D.C., Anderson, D.L. (Eds.), Plates, Plumes, and Paradigms. Geological Society of America Special Paper, vol. 388, pp. 463–476.
Sharma, K.K., 2007. K-T magmatism and basin tectonism in western Rajasthan, India, results from extensional tectonics and not from Réunion plume activity. In: Foulger, G.R., Jurdy, D.M. (Eds.), Plates, Plumes, and Planetary Processes. Geological Society of America Special Paper, vol. 430, pp. 775–784.
Shastry, A., Kumar, S., 1996. Trace and rare earth elements geochemistry of alkaline rocks of Sarnu-Dandali, Barmer, Rajasthan. Journal of Geological Society of India 48, 663–670.
Sheth, H.C., Choudhary, A.K., Bhattacharyya, S., Cucciniello, C., Laishram, R., Gurav, T., 2011. The Chogat-Chamardi subvolcanic complex, Saurashtra, northwestern Deccan Traps: geology, petrochemistry, and petrogenetic evolution. Journal of Asian Earth Sciences 41, 317–324.
Simonetti, A., Goldstein, S.L., Schmidberger, S.S., Viladkar, S.G., 1998. Geochemical and Nd, Pb, and Sr isotope data from Deccan alkaline complexes – inferences for mantle sources and plume-lithosphere interaction. Journal of Petrology 39, 1847–1864.
Snyder, D., 2000. Thermal effects of the intrusion of basaltic magma into a more silicic magma chamber and implications for eruption triggering. Earth and Planetary Science Letters 175, 257–273.
Srivastava, R.K., 1989. Alkaline and peralkaline rocks of Rajasthan. In: Leelanandam, C. (Ed.), Alkaline Rocks. Geological Society of India Memoir, vol. 15, pp. 3–24.
Subrahmanyam, N.P., Leelanandam, C., 1989. Differentiation due to probable initial immiscibility in the Musala pluton of the Mundwara alkali igneous complex, Rajasthan, India. Geological Society of India Memoir 15, 25–46.
Tewari, H.C., Dixit, M.M., Sarkar, D., 1995. Relationship of the Cambay rift basin to the Deccan volcanism. Journal of Geodynamics 20, 85–95.
Tibaldi, A., 2015. Structure of volcano plumbing systems: a review of multi-parametric effects. Journal of Volcanology and Geothermal Research 298, 85–135.
Udas, G.R., Narayan Das, G.R., Sharma, C.V., 1974. Carbonatites of India in relation of structural setting. Proceedings of international seminar on tectonics and metallogeny of south east Asia and far East, vol. 34. Geological Survey of India Miscellaneous Publication, pp. 77–95.
Upadhyay, D., Kooijman, E., Singh, A.K., Mezger, K., Berndt, J., 2015. The basement of the Deccan Traps and its Madagascar connection: constraints from xenoliths. Journal of Geology 123, 295–307.
Vanderkluysen, L., Mahoney, J.J., Hooper, P.R., Sheth, H.C., Ray, R., 2011. The feeder system of the Deccan Traps (India): insights from dyke geochemistry. Journal of Petrology 52, 315–343.
Verma, S.P., Torres-Alvarado, I.S., Sotelo-Rodriguez, Z.T., 2002. SINCLAS: standard igneous norm and volcanic rock classification system. Computers and Geosciences 28, 711–715.
Vermani, S., Gupta, A., Spitzer, W., Stolyarov, S., Arora, G., Dean, G., 2010. The Fracturing of Deep Non-conventional Volcanic Reservoir – a Case History: Raageshwari Gas Field, Onshore India. Society of Petroleum Engineers SPE132932.
Viswanathan, S., 1977. Differentiated dyke rocks of Mer Mundwara, Rajasthan and their metallogenic significance. Geological Magazine 144, 291–298.
Wilson, S.A., 2000. Data Compilation for USGS Reference Material BHVO-2, Hawaiian Basalt. United States Geological Survey Open File Report.
Winter, J.D., 2011. Principles of Igneous and Metamorphic Petrology, second ed. Prentice-Hall India, 701 pp.
Zellmer, G.F., Sheth, H.C., Iizuka, Y., Lai, Y.-J., 2012. Remobilization of granitoid rocks through mafic recharge: evidence from basalt-trachyte mingling and hybridization in the Manori-Gorai area, Mumbai, Deccan Traps. Bulletin of Volcanology 74, 47–66.